Bichromatic emission in a ring dye laser

N. M. Lawandy
Division of Engineering and Department of Physics, Brown University, Providence, Rhode Island 02912

R. Sohrab Afzal and W. S. Rabinovich
Department of Physics, Brown University, Providence, Rhode Island 02912
(Received 19 May 1986; revised manuscript received 16 January 1987)

We have performed an experimental study of a high-Q Rhodamine 6G ring dye laser and have measured bichromatic emission with wavelength spacings as large as 110 Å when the laser operated bidirectionally. The bichromatic emission vanished at all excitations when the laser was forced into unidirectional operation using a Faraday isolator. However, when a weak reflected beam was allowed to make a single pass in the direction opposite to that allowed by the Faraday device, bichromatic emission is recovered at the higher pump powers. The experiments show that no discontinuities occur in the intracavity power as a function of excitation and that the intracavity fields which are completely consistent with the measured thresholds are not capable of producing Rabi splittings larger than a few angstroms. In addition, we have observed no structure in the spontaneous emission spectrum of the dye when the bichromatic emission (80-Å splitting) was present in the laser mode. We have been able to quantitatively fit the threshold and wavelengths of the bichromatic emission using a distributed feedback mode analysis with a cavity-mode-induced susceptibility grating.

INTRODUCTION

Recently, there have been several theoretical and experimental studies of homogeneously broadened lasers which exhibit multichromatic emission. Theoretical conjectures which lead to multichromaticity are the self-pulsing behavior of the on-resonance Maxwell-Bloch equations (single-mode laser in the bad cavity limit with $\gamma_\parallel/\gamma_\perp < 0.20$), the good cavity Risken-Nummedal instability,[1,2] the interaction of semiclassical atoms with two intense laser modes in the good cavity limit, and the evolution of new mode solutions which find their origin in a distributed feedback mode generated by a cavity-mode-induced grating.[3,4]

Experimental investigations on the self-pulsing NH_3 laser have been performed which suggest that the $\gamma_\parallel/\gamma_\perp < 0.21$ regime has been found and that the heterodyne laser spectra are a verification of the single-mode theory.[5] It is not clear, however, that this regime is accessible since the required ratio of $\gamma_\parallel$ to $\gamma_\perp$ would be unlikely in a polar symmetric top molecule and the gain in these systems is not due solely to single-photon processes.[6,7]

Experimental observations of stable bichromatic emission in dye lasers have been reported by Hillman *et al.*[8] Other more recent work reporting similar results has also appeared.[9–11] The experiments report large bichromatic emission splittings (20–175 Å) and have been interpreted as being the effects of a strong two-mode interaction of a radiation field with a semiclassical atom. These effects require intensities on the order of 50 MW/cm^2 in order to achieve Rabi splittings of 50–80 Å. These values of intracavity powers are significantly higher than those one might expect to find in a single-transverse-mode dye laser pumped by a few watts of cw argon-ion laser power. Furthermore, the theory which is presented to account for the bichromatic emission[10] utilizes a T_1/T_2 ratio of 10 instead of the accepted value of 5×10^3.[12] Calculations of the susceptibility using the expressions derived in Ref. 10, the T_1/T_2 ratio of 5×10^3, and an intensity of 50 MW/cm^2 leads to only a central population pulsation dip of width T_1^{-1} in the usual power-broadend susceptibility curve.

In this paper we present experimental measurements on a high-Q Rhodamine 6G ring dye laser which was found to exhibit bichromatic emission with splittings on the order of 15–110 Å while operating in the range of 2–10 times above threshold in the bidirectional mode. The laser thresholds were lower than any reported in Refs. 8–11 indicating a higher Q in our system and the ability to further exceed the first laser threshold in our experiments. Experiments were performed with the insertion of a low-loss Faraday isolator (loss approximately 1.25%) in order to examine the effects of saturation gratings on the bichromatic emission. The results showed that the bichromatic emission was completely eliminated in the operating range 1–10 times above threshold.

When a weak reflection from an intracavity element was allowed to make a single pass through the active part of the jet in a direction opposite to that allowed by the Faraday rotator, bichromatic emission is recovered at high pump powers (5–7 W). This is believed to be a consequence of a Bragg grating which appears when the weak beam is sent through the active medium.

In addition, the side light fluorescence of the jet was spectrally examined in order to search for sideband splittings similar to those found in Na atoms in a strong resonant field.[13] Those splittings have been theoretically predicted for atoms interacting with resonant fields capable

of producing Rabi frequencies of the order T_2^{-1}.[14,15] No evidence of splittings or a fluorescence line-shape change was found when the laser was 2–10 times above threshold and exhibiting bichromatic emissions with 80-Å splittings. This we will show is consistent with the low powers measured in our cavity.

In the next sections we will describe the experiments, and the results which we obtained. In addition, we offer a theory based on a new mode-structure hierarchy which may explain our observations.

DESCRIPTION OF THE EXPERIMENTS

The experiments were carried out on a modified Spectra Physics 380 ring dye laser. The laser is a figure eight ring with a 200-μm-thick free-flowing dye jet of $2\times10^{-3}M$ solution of Rhodamine 6G in ethylene glycol. The jet is at the center of two curved mirrors which produce an average focused Gaussian beam spot radius of approximately 10–15 μm at the laser wavelength. In addition there is a pump focusing mirror which concentrates the argon-ion laser pump beam to a spot radius of about the same size as the laser mode beam waist. The multiline argon-ion pump laser is an actively power stabilized Spectra Physics Model 2020-05 with a range of 0–5 W. It should be noted, however, that over the course of the experiments, several new laser tubes were required. The new tubes were capable of delivering as much as 9 W of output for several days following installation. Each of the ring dye laser mirrors was controlled by two Starrett Inc. micrometers with ±2.0-μm positioning resolution.

The laser was operated in a totally sealed-off cavity containing only the dye jet, an astigmatism compensator (optional), and mirrors with the highest reflectivity coatings commercially available. The mirrors had a measured power transmitivity of $T=10^{-3.8}$ in the wavelength range 5700–6100 Å. The transmitivity of the mirror out of which the power measurement was made was measured at an angle of 8° (position in the cavity) against a National Bureau of Standards blank in a dry nitrogen pumped spectrophotometer. These values were obtained from absorbance measurements and therefore result in a maximum reflectivity. This is acceptable as we are interested in estimating the highest possible values for the intracavity fields. Using the measured output power in a given direction, the maximum possible intracavity power associated with that beam was directly found by dividing by the transmitivity factor $T=10^{-3.8}$. In addition to this technique, intracavity powers were measured using calibrated intracavity scattering. The measurements were performed in the presence of the average dusty environment using two overlapping copropagating beams (the intracavity laser beam and an external beam of known power).

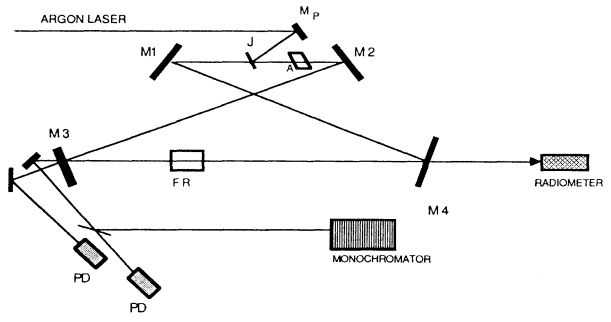

FIG. 1. Experimental apparatus for bichromatic emission: $M1,M2,M3,M4$ are laser cavity mirrors, 125 cm is the total cavity length, FR represents the Faraday isolator, PD the photodiode, A the astigmatism-compensating Brewster angle rhomb, J the dye jet, and M_P the pump focusing mirror.

Some of the experiments were performed with the insertion of a Faraday isolator to ensure unidirectional operation. The Faraday rotator had an insertion loss of about 1.25% which doubled the oscillation threshold pump power of the sealed-off cavity. The dye laser was modified with external reflectors to allow for the simultaneous monitoring of the wavelength output and the power coupled out in each direction of the ring. The wavelength measurements were performed using a Jarrel-Ash monochromator with a resolution of 1.5 Å and a S-20 photomultiplier tube. The measurements of the power coupled out were performed using two independently calibrated radiometers (Coherent 210 and Laser Precision RK3440 meter/RP538 head). In addition, fast *p-i-n* diodes were used to study the temporal output, in order to ensure that any bichromatic emission wavelengths observed were simultaneously present and not an instability phenomenon between wavelengths. The laser cavity and the external measurement hardware are shown in Fig. 1.

ANALYSIS OF THE DYE LASER ABOVE THRESHOLD

Among the critical parameters needed for the elucidation of the bichromatic state or any instability phenomenon are the gain and saturation behavior of the laser under study. A knowledge of the gain and the number of times above threshold the excitation produces are paramount to establishing an experimental correspondence between a theory and reality. The saturation behavior and in particular the saturation intensity are required to determine intramedium intensities. This is a critical parameter in our case if one is to discriminate between effects due to intense fields such as those claimed in Refs. 8–10 and other effects which lead to bichromatic emission.

The gain of conventional flowing dye jet dye lasers is known to be linearly proportional to pump power.[12,16] This behavior allows us to equate the ratio of unsaturated gain to the threshold gain to the ratio of pump power to threshold pump power. When only the astigmatism compensator (Brewster angle rhomb, 1% loss) was in the sealed-off cavity, the threshold pump power was found to be 0.35 W. This low threshold allowed us to access an excitation regime as large as ten times above threshold.

The measurement of output power versus pump power for the bidirectional dye laser operating with both the sealed-off cavity (5930 Å) and the conventional output coupler (3% output coupling at 6160 Å) are shown in Figs. 2(a) and 2(b). The output powers, spot size in the jet, and the ratio of pump power to threshold pump power imply that for the homogeneously broadened dye

laser, the saturation intensity of the dye is of the order of 250 kW/cm^2.

This value is in good agreement with many models of dye lasers. Typical five-level models give values of the order of 400 kW/cm^2 which when refined to include the excited singlet-singlet absorption lead to values of the order of 300 kW/cm^2.[12] A detailed experimental study of our ring dye laser with retroreflection and the myriad of theoretical treatments of dye lasers indicate that typical flowing dye jet lasers (rhodamine 6G) have intensity-gain-length products on the order of $(0.04-1.5)P$ where P is the argon laser pump power.[16] With these values one would have to have a laser with less than 0.3% losses. This requirement alone would require an environment with less than ten dust particles per cubic centimeter in the optical path.[17] In view of these arguments it would be extremely difficult for a sealed-off rhodamine ring dye laser pumped by a few watts of pump power from an argon-ion laser to produce more than 1–3 W of intracavity power and medium intensities greater than 1–5 MW/cm^2.[18]

In the next section we will show that the measured intracavity power of our sealed-off dye laser, which has exhibited dramatic bichromatic splittings in a low-order Gaussian mode, is consistent with the arguments we have presented.

EXPERIMENTS ON THE INTRACAVITY POWER OF THE SEALED-OFF RING LASER

Experiments were performed to measure the intracavity power of the sealed-off ring laser as a function of excitation when it was operating in the lowest-order Gaussian transverse mode. Two measurement methods were utilized to obtain the intracavity circulating power: (1) direct radiometric measurements of the transmitted output beam and (2) calibrated intracavity scattering using overlapping reference and ring laser beams.

The output power from the sealed-off cavity was quite low and had to be measured radiometrically. The output powers emitted through the characterized mirror described in the previous section ranged from 10–600 μW. Using the measured total transmitivity (including scattering and absorption) of the mirror, we were able to estimate the maximum obtainable circulating intracavity powers to be of the order of 3 W. Figs. 3(a) and 3(b)

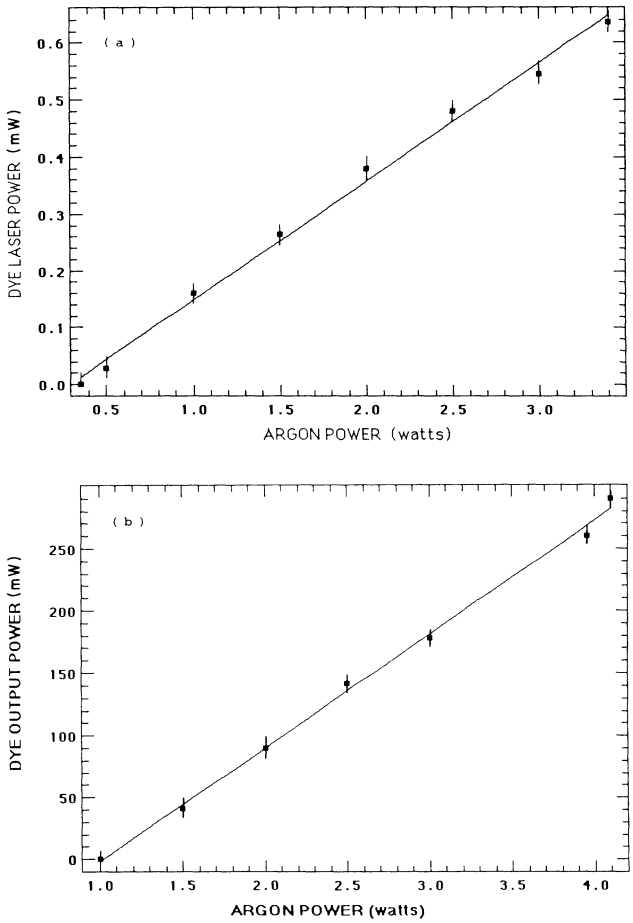

FIG. 2. Dye output power vs pump power (a) with sealed cavity (0.016% transmission) and (b) with output coupler as $M4$ (3% transmission).

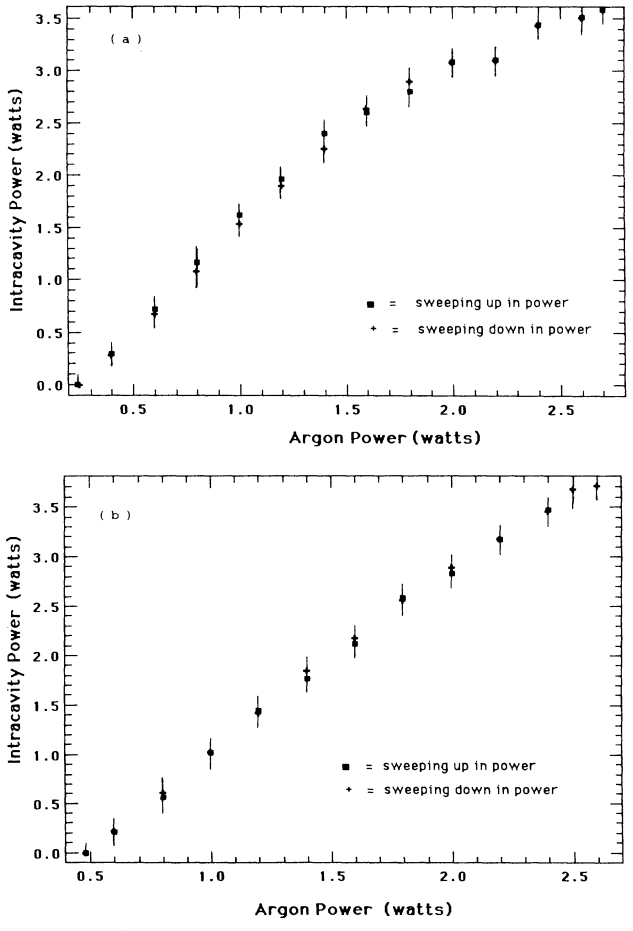

FIG. 3. Intracavity power vs pump power as calculated using output power and measured transmitivity for the sealed-off cavity (a) operating bidirectionally and (b) operating unidirectionally with the insertion of a Faraday isolator.

show the maximum intracavity power as a function of pump power for the case of bidirectional and unidirectional operation, respectively, at a wavelength of 5890 Å. The cycling up and down of the input pump power showed no discontinuities and revealed no hysteresis within the resolution of the experimental measurements.

A separate, more direct measurement of the intracavity power was performed using light scattering. The measurement was undertaken with the normally present *dusty* environment of the laser cavity using two overlapping beams. One beam from the argon laser served as a calibration beam while the other was the intracavity beam under investigation. This technique enables us to measure both the reference and signal beam without realignment of the measuring apparatus and also allows for the same scattering particles (dust) to interact with both beams. The experiment utilized for the direct scattering measurements is shown in Fig. 4. It should be pointed out that such a time-averaged measurement is likely to be more accurate than Rayleigh scattering since a complete removal of dust is required to have a reasonable calibration between any external measurement and an internal measurement.[19]

The results of the scattering measurements indicated intracavity circulating powers which were of the same order of magnitude but always smaller than those found from the external power measurements. This is satisfying in view of the previously stated fact that the transmitivity measurement of the reflector only serves to generate an upper bound on the Q of the cavity.

With 2.4 W of pump power (threshold in this case was 0.5 W) and a calibration beam power of 0.48 W, the raw data indicated an internal power of 0.48 W at the dye laser wavelength circulating inside the cavity. This value must be corrected by the relative 90° Mie scattering cross-section dependence on wavelength since the calibration beam is at 4880 Å and the laser emission is at 5970 Å.[17] The correction factor assuming an average dust particle diameter of 20 μm leads to a factor of 1.3 and an increase in the circulating laser power, bringing the intracavity power to a value of 0.62 W. This value is consistent with the measurements performed by transmission as this intracavity power and a transmitivity of $10^{-3.8}$ leads to external powers on the order of 100 μW.

These measurements show that the two independent methods of measuring the intracavity power are consistent and indicate that there can be at most 1–3 W in our sealed-off dye cavity excited by pump powers of the order of a few watts (0–6). Furthermore, we have seen no evidence of discontinuities in the power of the dye laser as a function of excitation. In the next section we will show that these powers are completely consistent with the saturation intensities of 100–400 kW/cm^2.

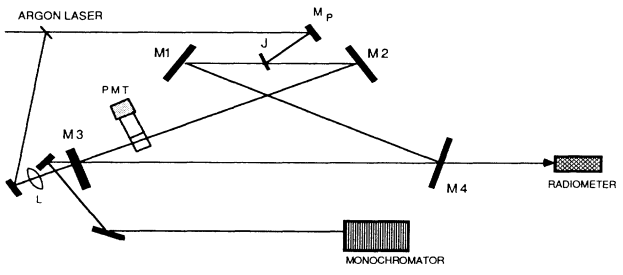

FIG. 4. Experimental apparatus to measure intracavity power from scattering: $M1,M2,M3,M4$ are laser cavity mirrors, 125 cm is the total cavity length, L represents the Argon laser reference beam focusing lens (focal length 40 cm), PMT the photomultiplier tube, J the dye jet, and M_P the pump focusing mirror.

BICHROMATIC EMISSION EXPERIMENTS WITH BIDIRECTIONAL OPERATION

The Rhodamine 6G dye laser output was examined spectrally with a resolution of 1.5 Å. The laser output

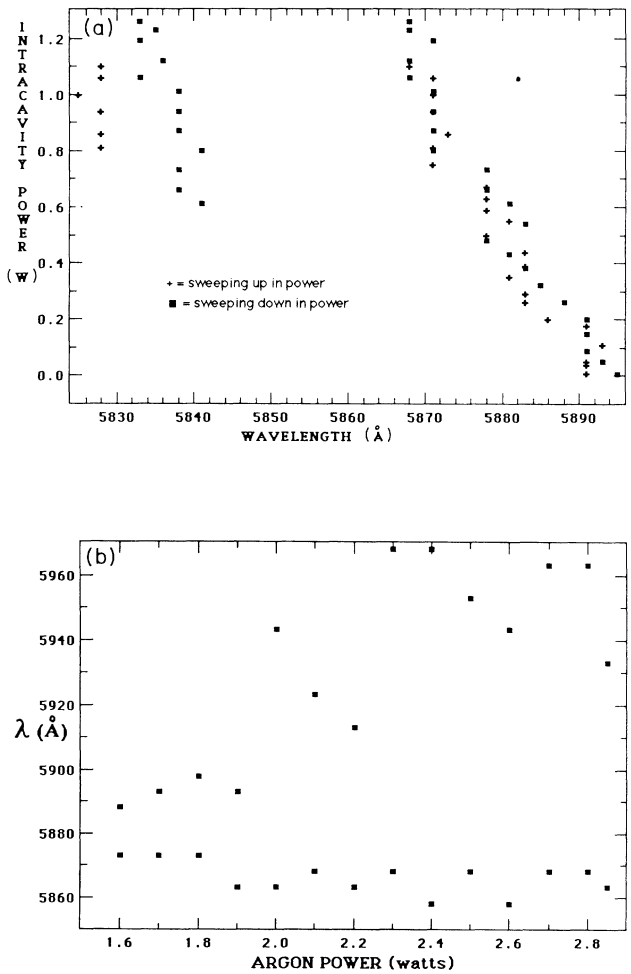

FIG. 5. (a) Bichromatic splitting vs intracavity power. (b) Same as (a) but with altered intracavity dispersion.

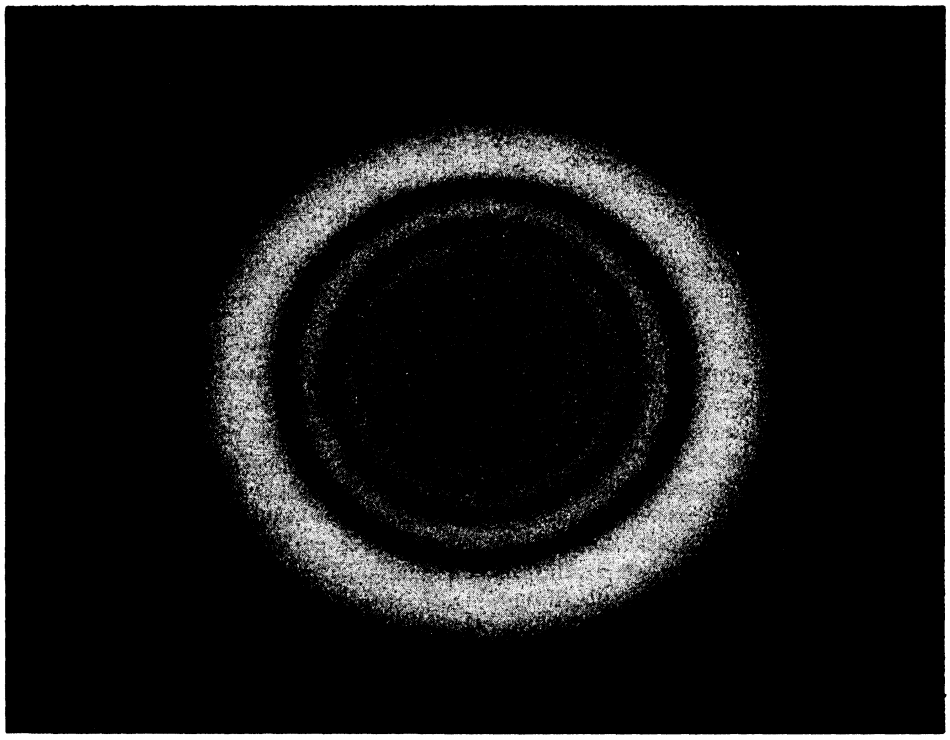

FIG. 6. Newton's rings formed by the thermal lensing effect when the laser was in its lowest-order transverse mode and operating bidirectionally with an 80-Å splitting.

was sent through a diffuser before entering the monochromator in order to eliminate any spatial ghost effects which could appear as spectral structure. The results of a typical experiment to measure the spectral output versus intracavity power are shown in Figs. 5(a) and 5(b). The measurements in Fig. 5 were undertaken in order to measure the bichromatic separation as well as to search for chromatic hysteresis. Within the resolution of the experiments we were able to measure large splittings but again found no evidence of hysteresis. Figure 5(b) shows bichromatic emission when slight changes in the intracavity dispersions are affected. This type of sensitivity to dispersion has also recently been reported by Koch *et al.*[20]

In order to ensure that the laser was operating in a single transverse mode at all times (including the regime of bichromatic behavior), qualitative and quantitative measurements of the transverse-mode profile were performed. Qualitatively, the intensity pattern was studied using the

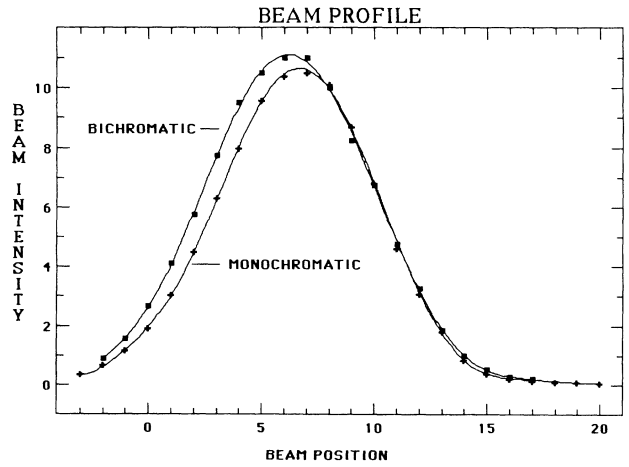

FIG. 7. Transverse beam profile with and without bichromatic output.

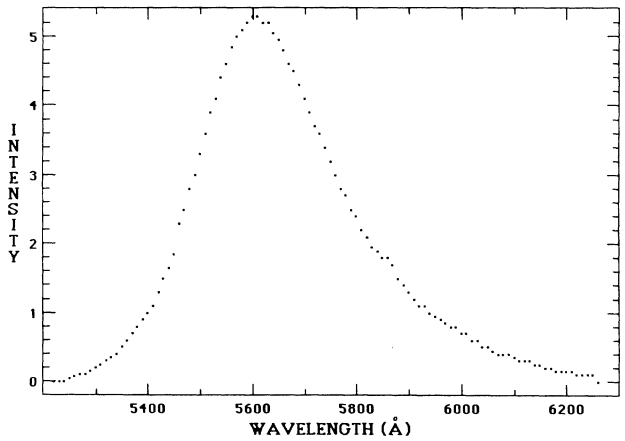

FIG. 8. Resonance fluorescence spectrum with a bichromatic splitting of 80-Å on the laser mode.

Newton's rings which formed when the output beam traversed a thermal lensing plastic. The rings which reflect a high degree of mode symmetry are shown in Fig. 6. In addition, the far-field transverse-mode profile of the laser was scanned with the laser operating monochromatically and with the laser operating bichromatically. The superimposed transverse-mode profiles are shown in Fig. 7.

EXPERIMENTS WITH FORCED UNIDIRECTIONAL OPERATION

In order to unambiguously test for the effects of saturation gratings on the bichromatic emission, we operated the high-Q ring laser with an intracavity antireflection-coated Faraday isolator to force unidirectional operation. When the laser was operated with the Faraday isolator and the astigmatism-compensating Brewster angle rhomb, the threshold pump power increased to about 0.7 W. These experiments were operated with as much as 9 W of pump power bringing the laser to an excitation which is 12 times above threshold. In every experiment that we performed with forced unidirectional operation, there was *no bichromatic emission.*

When an intracavity glass surface was used to reflect the strong unidirectional beam in the counterpropagating direction for a single pass through the active dye region, bidirectional emission occurred at high pump powers (≥ 5 W). When the weak reflected beam was slightly misaligned, the bichromatic emission vanished. Measurements of the power of the counterpropagating beam verified that it was only seeing the saturated single-pass gain of the jet. These experiments clearly demonstrate that saturation gratings are necessary and are likely to be at the heart of the bichromatic state observed in our experiments.

As an additional test of the bichromatic state induced by an atom in a strong field, we examined the fluorescence of the jet in order to check for structures similar to that observed in sodium vapor experiments.[13] The fluorescence spectrum was identical when the laser was running unidirectionally with the higher circulating power and when it was operating bidirectionally and exhibiting an 80-Å bichromatic emission on the laser mode. The fluorescence spectrum was void of structure and is shown in Fig. 8. This result is not surprising since the actual intracavity powers could only produce Rabi splittings on the order of a few angstroms.

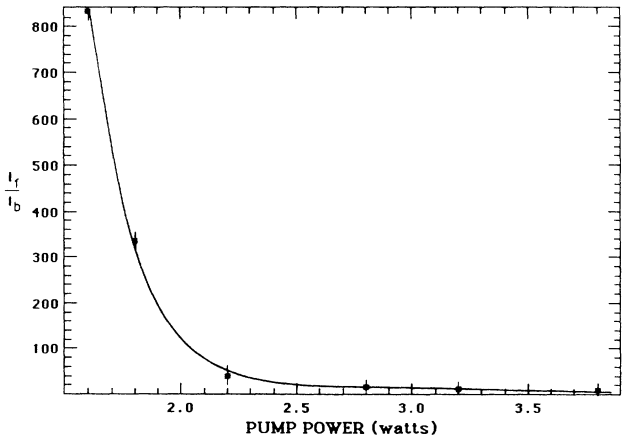

FIG. 9. Ratio of counterpropagating intensities as a function of pump power for the laser with retroreflection. The laser was operating at 6000 Å with an output coupling of 7%.

INDIRECT MEASUREMENTS OF THE SUSCEPTIBILITY GRATINGS

The experiments we have reported previously in the text clearly indicate that the bichromatic state is a consequence of effects associated with simultaneous counterpropagating coherent beams. In particular, they do not necessarily require two counterpropagating ring laser modes but simply two counterpropagating waves, one of which is the laser mode. Motivated by the results of the previous experiments, we measured the counterpropagating intensities of the bidirectionally operating ring laser.

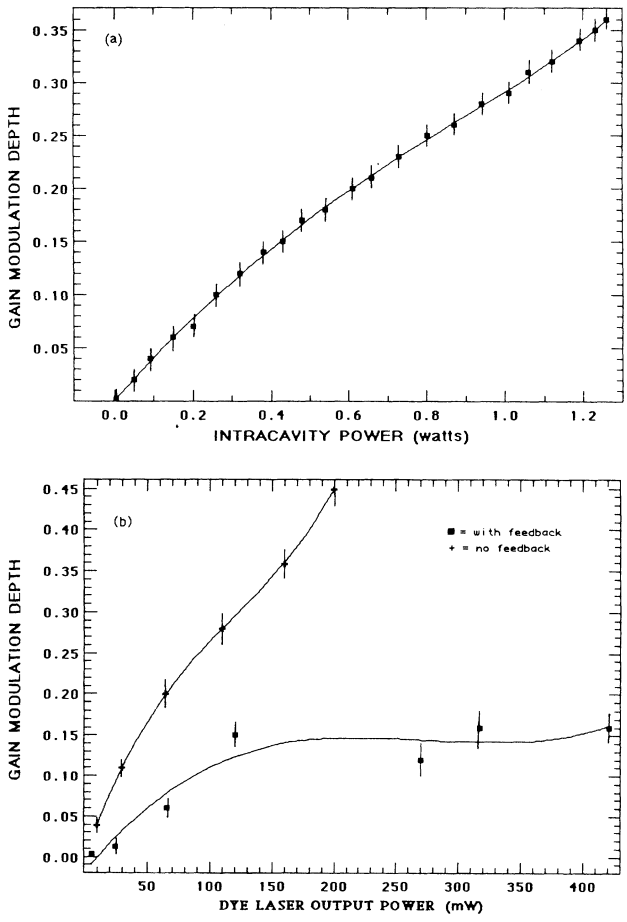

FIG. 10. (a) The gain-length modulation of the gain medium vs intracavity power for the sealed-off ring laser. The gain-length modulation is calculated from the intensity with the normal saturation expression at line center. (b) Gain-length modulation vs output power with and without retroreflection.

In addition, we measured the counterpropagating intensities in the presence of a retroreflecting external mirror. This was done in order to understand the reported results of bichromatic emission with retroreflection.[11]

The experiments measuring the two intensities were equal to within ±15% unless a retroreflector was present. The retroreflection measurements were performed with an output coupling of about 5% while all other measurements were performed using a sealed-off cavity. The ratio of the intensities with retroreflection was large near threshold but decreased sharply when the laser excitation was increased due to unavoidable coupling of the counterpropagating waves by intracavity scattering.[21] Figure 9 shows the counterpropagating intensity ratio as a function of pump power for the laser with retroreflection. At any time throughout the experiment, if the retroreflection was blocked both beams reappeared with equal intensity, indicating that a field was always present at the retroreflector. Furthermore, when the retroreflecting mirror was moved back a narrow region of oscillation was observed.[22]

Using the measured intensities we were able to infer the intensity pattern in the jet in the limit that the counterpropagating modes have the same wave vector and frequency. These values were then used to calculate a gain-length modulation depth (gain modulation depth multiplied by active medium length) as a function of the circulating power in one direction from a standard saturation expression for a two-level atom in a resonant field. The results of the experimentally inferred gain-length modulation as a function of intracavity power for the sealed-off bidirectional laser (no feedback) are shown in Fig. 10(a). Figure 10(b) shows a comparison of the gain-length product for a 7%-output coupling laser with and without feedback. Detailed experimental studies of the intensity and gain gratings in a ring dye laser with retroreflection were also performed at several wavelengths and cavity configurations.[21]

This set of experiments verifies that large gain-length modulations are present in the bidirectional ring laser. Furthermore, we have shown that the retroreflection effect in a dye ring laser does not totally eliminate the counterpropagating wave. In addition the gain-length gratings with retroreflection increase as the laser is brought to higher excitations and are comparable to those without retroreflection. These experimental results indicate that retroreflection significantly eliminates saturation gratings in dye lasers only near threshold.

TOWARDS A THEORY OF BICHROMATIC EMISSION

In the following section we examine the effect of the intensity-induced Bragg grating on the mode structure that occurs in a bidirectional ring laser. The standing wave that occurs due to the growth of the bidirectional ring cavity modes creates a saturation-induced grating in the susceptibility of the dye which has precisely the right periodicity to couple waves with frequencies within the linewidth of the dye. Thus, the original ring cavity modes induce a distributed feedback (DFB) medium in the ring cavity and create a new mode structure in which ring-DFB modes may reach threshold within the operating range of a low-loss dye laser. The steady-state threshold mode structure results in coexisting modes that are spaced by tens of angstroms. This we suggest is the origin of the bichromatic state. The stability of these modes beyond the first laser threshold is also studied using a Fourier decomposed rate equation model. The coupling terms in the dynamic model are based upon threshold longitudinal mode profile solutions found in the steady-state results.

THRESHOLD MODE RESULTS

Previous work on the effects of counterpropagating fields have focused on the coupling of ring cavity modes by the grating using constant spatial envelopes for the modes.[23–25] Work by Kogelnik and Shank,[26] Chinn,[27] Streifer, Burnham, and Scifres,[28] and Rabinovich and Lawandy[29] have shown that to correctly describe the modes of a periodically modulated medium it is necessary to use spatially varying envelopes for the fields. Among the effects that are lost when the mode envelopes are forced to be constant are thresholds that depend upon the grating size, the formation of a forbidden gap at the Bragg frequency, and mode spacings that depend upon both the cavity length and the length of the medium. In this section we present results on the threshold longitudinal mode structure of a periodically modulated medium with a finite linewidth in a partially filled ring cavity.

The solutions derived are an extension of the coupled mode theory of Kogelnik and Shank[26] and include the effects of the molecular line shape. This extension is somewhat different in form to that of Sargent *et al.*[30] but has similar content. The full derivation of these equations is given in Ref. 29, but we will sketch the derivation here.

We start with the scalar wave equation

$$\partial^2 E/\partial z^2-(n^2/c^2)\partial^2 E/\partial t^2=\mu_0\partial^2 P/\partial t^2 , \tag{1}$$

where E is the electric field and P the polarization. We set

$$P=\epsilon_0\chi(\omega)E \tag{2}$$

and assume a periodically modulated frequency-dependent susceptibility $\chi(\omega)$:

$$\chi(\omega)=\chi_0(\omega)[1+m\cos(2\beta_0 z)] , \tag{3}$$

where m is a parameter controlling the depth of the modulation of the medium. The electric field is assumed to have the form

$$E(z)=R(z)\exp(-i\beta_0 z)+S(z)\exp(i\beta_0 z) , \tag{4}$$

where $R(z)$ and $S(z)$ are slowly varying envelopes. $\beta_0=2\pi/\lambda_0$ and λ_0 is the Bragg wavelength. Further manipulation results in the coupled-mode equations for the field envelopes:

$$-R'+\{\alpha_0 g(\delta-\delta_a)-i[\delta+\alpha_0 h(\delta-\delta_a)]\}R = i(m/2)[\alpha_0 h(\delta-\delta_a)+i\alpha_0 g(\delta-\delta_a)]S , \tag{5a}$$

$$S'+\{\alpha_0 g(\delta-\delta_a)-i[\delta+\alpha_0 h(\delta-\delta_a)]\}S = i(m/2)[\alpha_0 h(\delta-\delta_a)+i\alpha_0 g(\delta-\delta_a)]R , \tag{5b}$$

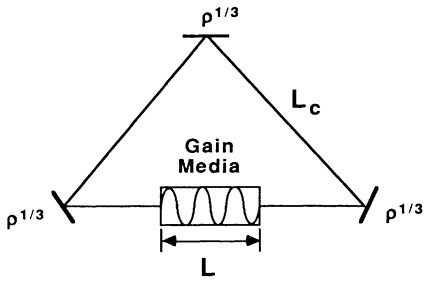

FIG. 11. Schematic of the ring laser model used for the cavity-mode-induced bulk mode theory.

where α_0 is the gain at line center, δ is the detuning of the field from the Bragg frequency, δ_a is the detuning of the molecular line center from the Bragg frequency, $g(\delta-\delta_a)$ is a normalized Lorentzian line shape for the imaginary part of the susceptibility, and $h(\delta-\delta_a)$ is a normalized line shape for the real part of the susceptibility. We define the grating height κ as $(m/2)[\alpha_0 h(\delta-\delta_a)+i\alpha_0 g(\delta-\delta_a)]$. κ is identical with the DFB coupling.[26]

Next we apply ring boundary conditions to the fields. A general solution to the coupled mode equations can be written as

$$R(z)=r_1 e^{\gamma z}+r_2 e^{-\gamma z}, \tag{6a}$$

$$S(z)=s_1 e^{\gamma z}+s_2 e^{-\gamma z}, \tag{6b}$$

where r_1, r_2, s_1, and s_2 are complex constants and γ is the DFB eigenvalue. Then we set

$$(r_1 e^{-\gamma L/2}+r_2 e^{\gamma L/2})=\rho'(r_1 e^{\gamma L/2}+r_2 e^{-\gamma L/2}), \tag{7a}$$

$$(s_1 e^{\gamma L/2}+s_2 e^{-\gamma L/2})=\rho'(s_1 e^{-\gamma L/2}+s_2 e^{\gamma L/2}), \tag{7b}$$

where

$$\rho'=\rho e^{-i(\beta_0+\delta)(1/f-1)L-i\beta_0 L}. \tag{8}$$

ρ is the lumped reflectivity of the cavity, L is the length of the medium, and f is the filling factor of the cavity. Using these boundary conditions an eigenvalue relation for γ can be found:

$$\gamma L=\frac{\pm\iota\kappa L\sinh(\gamma L)(1-\rho'^2)}{(1-\rho' e^{\gamma L})(1-\rho' e^{-\gamma L})}. \tag{9}$$

Knowing γ, we can predict the threshold gain, mode frequency, and longitudinal mode patterns of the modes of a ring-distributed feedback medium.

In addition we find a transcendental relation for the threshold gain:

$$\alpha L=\iota\kappa L\left[\frac{(1+\rho'^2)\cosh(\gamma L)-2\rho'}{1+\rho'^2-2\rho'\cosh(\gamma L)}\right]. \tag{10}$$

We have used these results to study the threshold mode structure of the ring dye laser (Fig. 11). The lineshape functions $g(\delta-\delta_a)$ and $h(\delta-\delta_a)$ use a dye linewidth of approximately 250 Å. The gain α_0 is a function of pump power and is determined using accepted rate equation models for Rhodamine 6G.[12] The modulation parameter m, which sets the size of the induced grating, is determined using the measured values of the counterpropagating waves and the known saturation intensity of Rhodamine 6G.[12] In addition, a dispersive loss modeled as a frequency dependence in ρ is used to make the peak gain minus loss occur approximately 60 Å off line center. Experimentally we find that the laser oscillates 60 Å off line center due to weak dispersion in the cavity because of the astigmatism device. The frequency dependence in ρ is an attempt to model this fact. The loss has a constant component and a Lorentzian component with a line shape having a full width at half maximum of 300 Å and a height of 6%. The minimum loss near where the ring cavity mode oscillates is 4% and is 66 Å above line center. The length of the cavity is 1.1 m and the length of the active medium is 80 μm.

Using these parameters in the ring-DFB model, we have found several important characteristics of the ring-DFB modes in our laser. The mode spacing in a ring-DFB system is determined by the length of the cavity, the length of the medium, and the relative sizes of the grating reflection to mirror reflection. Due to the extremely low

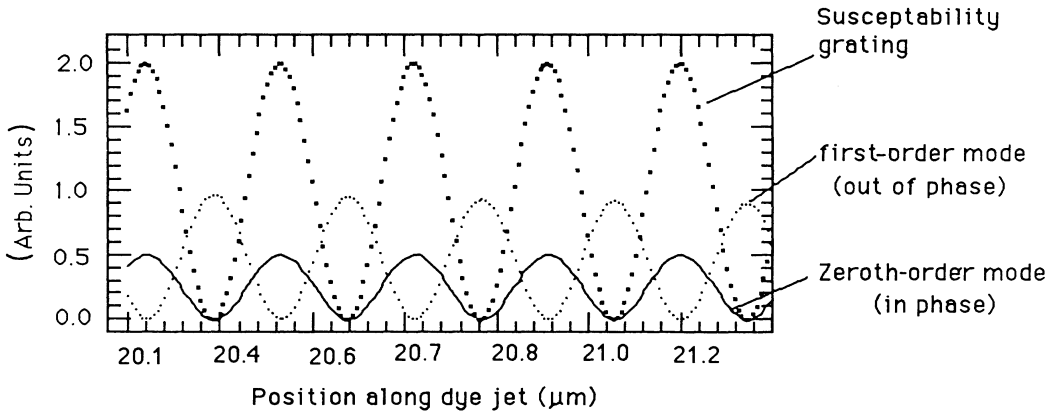

FIG. 12. Rapidly varying longitudinal mode intensity pattern for the susceptibility grating, zeroth-order ring-DFB mode, and first-order ring-DFB mode.

filling factor of our laser, the ring cavity modes are packed much more densely than the pure DFB modes (by roughly $L_c/2L$ or about 10 000 to 1). Hence there is a ring cavity mode very near each DFB mode and the mode spacing for the ring-DFB modes is determined by the length of the active gain medium rather than that of the cavity. The mode spacing is approximately 1.5 THz or about 10 Å due to the short length of the medium. This is on the order of the smallest observed bichromatic splittings. The longitudinal mode patterns have also been found and show that the zeroth-order mode is nearly flat in profile, but oscillates in phase with the grating and so is a "hole filling mode." As this mode passes threshold it saturates the grating and so cannot support a grating on its own. The higher-order modes tend to alternate being out of phase and in phase with the grating. The first-order mode, for instance, is out of phase with the grating, like the original grating-inducing ring cavity modes. The longitudinal mode envelope of the first-order mode is not flat but peaked in the center. Once the out-of-phase modes grow, they increase the grating and thus can support a grating on their own. The rapidly varying part of the zeroth-order mode, the first-order mode, and the gain are shown in Fig. 12.

Further, the threshold of these modes depends not only on the cavity feedback but also on the size of the grating, κ. The zeroth-order mode's threshold is strongly affected by the grating, while higher-order modes are much less strongly affected. As the gain in the system is increased, the grating grows and the threshold for these ring-DFB modes is lowered. We have defined the turn-on threshold pump power for these modes as that at which their grating-dependent threshold gains minus the loss at their mode frequency equal the threshold gain minus loss of the original ring cavity modes. The detuning from the Bragg grating and thresholds for the ring-DFB modes are shown in Fig. 13.

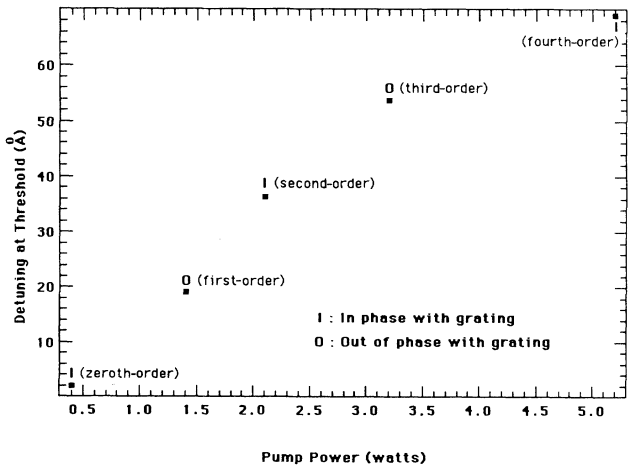

FIG. 13. Theoretical bichromatic splitting vs pump power as predicted by the ring-DFB theory.

DYNAMICS ABOVE THRESHOLD

While a full description of the dynamics and modal stability of the bidirectional ring laser requires a numerical solution of the partial differential equations that describe the system, some insight can be gained by using the steady-state results we have obtained to create a simpler model for the system. As soon as the original bidirectional ring cavity modes grow and create a grating, the mode structure is altered to that described in the previous section. The modes in the dye laser are now ring-DFB modes instead of simply ring cavity modes. It should be pointed out that these modes, while having different frequencies, all have the same spacing in their rapidly varying component. That is, all the ring-DFB modes are modulated at the Bragg wavelength and thus may induce gratings at the Bragg wavelength. The zeroth-order mode is the one that has its threshold lowered the most by the presence of a grating; however, it is in phase with the grating and thus cannot induce a grating on its own. We then expect that infinitesimally above threshold the first-order, out-of-phase, ring-DFB mode is the only one present. Since this mode is modulated in the same way as the original ring cavity modes and has a threshold only weakly dependent on the grating, it is essentially indistinguishable from bidirectional ring cavity modes in a non-modulated medium. As the gain in the system is raised and the grating increases, the threshold for the zeroth-order hole-filling ring-DFB mode drops until it is above threshold and can grow. This leads to a bichromatic state with a spacing of about 19 Å.

We have modeled the interaction between the in-phase and out-of-phase modes which lead to bichromatic emission using a system of rate equations. The full derivation of this model is given in Ref. 4; a sketch is given here. The steady-state results show that for a wide range of parameters the lowest-order ring-DFB mode is well approximated:

$$E_d(z,t)=E_d(e^{-\iota(\beta z+\Omega/2)}+e^{\iota(\beta z+\Omega/2)})e^{\iota\omega_d t}+\text{c.c.}\ , \tag{11}$$

where E_d is the mode amplitude, ω_d is the angular frequency of the ring-DFB mode, and Ω is an adjustable phase angle that we tie to the phase of the grating to ensure that the zeroth-order mode stays out of phase with the gain grating, where the induced gain grating can be written in the form $2\kappa\cos(2\beta z+\Omega)$. In our formulation we have decomposed the grating into a cosine component $\alpha_{g1}\cos(2\beta z)$ and a sine component $\alpha_{g2}\sin(2\beta z)$, where α_{g1} and α_{g2} are the amplitudes of these components. Ω is then determined dynamically as $\Omega=\cos^{-1}[\alpha_{g1}/(\alpha_{g1}^2+\alpha_{g2}^2)^{1/2}]$. Thus when the spatially modulated portion of the gain is, for instance, a cosine with positive amplitude (α_{g1} positive and finite, α_{g2} zero), Ω is equal to 0. As the grating changes due to saturation, its phase may change, and by tying Ω to the phase of the grating we ensure that the modulation of the ring-DFB mode intensity maintains a constant phase difference with respect to the grating as it is required to by the ring-DFB coupled-mode equations.[29]

The threshold gain for the zeroth-order ring-DFB mode can be found using Eq. (10). We can approximate this relation by expanding the cosh to second order in γL and using the DFB dispersion relation for a gain coupled distributed feedback laser on resonance:

$$(\gamma L)^2=(\alpha L)^2-(\kappa L)^2 \ . \tag{12}$$

The resulting cubic equation can be solved to yield an analytic approximation for the threshold gain as a function of mirror reflectivity and grating height:

$$\alpha_{\rm th}L=\{(\rho'-1)[(\kappa L)^2(\rho'^2-2+1)+16\rho']^{1/2} +\kappa L(\rho'^2+2\rho'+1)\}/4\rho' \ . \tag{13}$$

This approximation is very good for coupling strengths κL less than one which is always true for our laser. This threshold gain can be used to define a cavity decay rate for the zeroth-order ring-DFB field.

The first-order ring-DFB modes that are out of phase with the grating are modeled as $E_m(z,t)=E_m(e^{-\iota\beta z}-e^{\iota\beta z})e^{\iota\omega_m t}+$c.c. The threshold for this mode is assumed independent of the grating, which is approximately true for small gratings.

Using the assumed forms of the fields, we can find the longitudinal intensity pattern in the medium. This pattern consists of a constant term and the harmonics at twice the Bragg frequency that provide the grating. We write the gain as

$$\alpha(z)=\alpha_c+\alpha_{g1}\cos(2\beta z)+\alpha_{g2}\sin(2\beta z) \ . \tag{14}$$

As I/I_s gets much larger than one, higher spatial harmonics also becomes important. The size of the gain grating, κ, is a dynamic quantity defined in terms of the variables in the rate model as $|\kappa|=\frac{1}{2}(\alpha_{g1}^2+\alpha_{g2}^2)^{1/2}$. This equivalent to the definition of κ used earlier.

Since dye lasers have a large polarization decay rate, we are able to adiabatically eliminate the polarization and use a rate equation approach. In the rate equation limit we find, by projecting out the individual Fourier components, the following five rate equations for the system:

$$\dot{E}_m=\left[\frac{c\alpha_c f_m L}{L_c}-\tau_m^{-1}\right]E_m \ , \tag{15}$$

$$\dot{E}_d=\left[\frac{c\alpha_c f_d L}{L_c}-\tau_d^{-1}(\alpha_{g1},\alpha_{g2})\right]E_d \ , \tag{16}$$

$$\dot{\alpha}_c=-\frac{\Gamma}{2}\left[2E_dE_m(\hat{\mathbf{e}}_d\cdot\hat{\mathbf{e}}_m)\sin(\Delta\omega t)\left[\alpha_{g1}\sin\frac{\Omega}{2}-2\alpha_c\sin\frac{\Omega}{2}+\alpha_{g2}\cos\frac{\Omega}{2}\right]-\alpha_{g2}E_d^2\sin\Omega+\alpha_{g1}E_d^2\cos\Omega -\alpha_{g1}E_m^2+2\alpha_cE_m^2+2\alpha_cE_d^2+2\alpha_c-2\alpha_0\right] \ , \tag{17}$$

$$\dot{\alpha}_{g1}=-\Gamma\left[2e_dE_m(\hat{\mathbf{e}}_d\cdot\hat{\mathbf{e}}_m)\sin(\Delta\omega t)\left[\alpha_c\sin\frac{\Omega}{2}-\alpha_{g1}\sin\frac{\Omega}{2}\right]+\alpha_cE_d^2\cos\Omega+\alpha_{g1}E_m^2-\alpha_cE_m^2+\alpha_{g1}E_d^2+\alpha_{g1}\right] \ , \tag{18}$$

$$\dot{\alpha}_{g2}=-\Gamma\left[2E_dE_m(\hat{\mathbf{e}}_d\cdot\hat{\mathbf{e}}_m)\sin(\Delta\omega t)\left[\alpha_c\cos\frac{\Omega}{2}-\alpha_{g2}\sin\frac{\Omega}{2}\right]-\alpha_cE_d^2\sin\Omega+\alpha_{g2}E_m^2+\alpha_{g2}E_d^2+\alpha_{g2}\right] \ , \tag{19}$$

where Γ is the population relaxation rate, α_0 is the small-signal gain, τ_m^{-1} is the out-of-phase ring-DFB-mode decay rate defined in the normal manner, τ_d^{-1} is the cavity decay rate of the in-phase ring-DFB mode calculated from the approximation of the threshold gain; it is a function of the grating size. L_c is the length of the cavity. f_m and f_d are numerical factors to account for the frequency position of the out-of-phase and in-phase modes, respectively, in the gain line shape, and $\hat{\mathbf{e}}_d$ and $\hat{\mathbf{e}}_m$ are the unit vectors in the direction of the polarization of the out-of-phase and in-phase ring-DFB modes, respectively. Dispersive losses can be accounted for by using different values of ρ for the first- and zeroth-order ring-DFB-mode-cavity decay rates.

We have numerically integrated these equations for the parameters in our laser. The evolution of the zeroth-order, in-phase, ring-DFB mode and the first-order, out-of-phase, ring-DFB mode can be seen in Fig. 14. The first-order mode grows first creating a grating

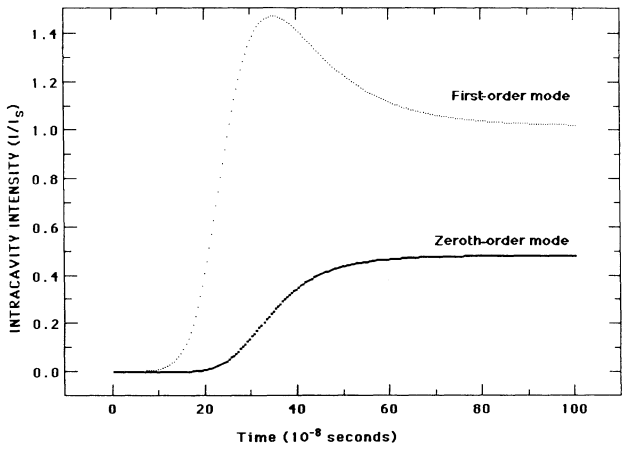

FIG. 14. Dynamic evolution of the stable bichromatic state.

that lowers the threshold of the zeroth-order mode. This mode begins to grow and saturate the average gain. The growth of this mode reduces the gain available for the first-order mode and it begins to drop in intensity, reducing the size of the grating. The growth of the zeroth-order mode also reduces the grating size increasing its own threshold. Eventually a steady state is reached in which the gain minus loss of both the first-order and zeroth-order ring-DFB modes are zero. Thus the dynamic nature of the threshold of the ring-DFB modes allows the system to automatically adjust itself so that two modes can be above threshold simultaneously even in a homogeneously broadened system. The large bichromatic splitting is the result of the new mode structure created in the active distributed feedback resonator, which owing to its short length (80 μm) produces very widely separated coexisting modes.

CONCLUSIONS

We have performed a careful experimental study of a high-Q Rhodamine 6G ring dye laser and have measured stable bichromatic emission with wavelength separations as large as 110 Å when the laser was operating *bidirectionally.* The experiments show that the measured intracavity fields *are completely consistent with the measured thresholds,* and saturation intensity, and are *not capable* of producing Rabi splittings larger than a few angstroms. Measurements of the intracavity power as a function of pump power exhibited no discontinuities or hysteresis. Most importantly, the bichromatic emission vanishes at all excitations when the laser is forced into unidirectional operation using a Faraday isolator.

When a weak reflected beam was allowed to make a single pass in the direction opposite to that allowed by the Faraday device, bichromatic emission was recovered at the higher pump powers. In addition, experiments were performed to examine the resonance fluorescence spectrum of the dye. The results showed that no Rabi sidebands were present when the laser mode exhibited an 80-Å bichromatic emission. These experiments show, we feel, that support for a susceptibility grating is required in the medium to observe the bichromatic state.

We have been able to quantitatively fit the threshold and wavelengths of the bichromatic emission using a ring-distributed feedback mode analysis. The success of the threshold analysis indicates that a new mode structure hierarchy exists in the dispersive multimode bidirectional, high-Q ring laser. Finally, we have shown using a Fourier decomposed rate equation system that owing to the phase relationship between the ring-DFB mode's that there exist stable bichromatic solutions based on the longitudinal mode profiles we have found.

ACKNOWLEDGMENTS

N. M. Lawandy is grateful to the National Science Foundation (Grant No. NSF-ENG-8451099), the Alfred P. Sloan Foundation, and NASA (NAG 5-526) for support of this work.

[1]L. M. Narducci, H. Sadiky, L. A. Lugiato, and N. B. Abraham, Opt. Commun. **55**, 370 (1985).

[2]H. Risken, *Optical Instabilities,* Vol. 4 of *Cambridge Studies in Modern Optics,* edited by R. W. Boyd, M. G. Raymer, and L. M. Narducci (Cambridge University Press, Cambridge, England, 1986), p. 20.

[3]N. M. Lawandy and W. S. Rabinovich, *Optical Instabilities,* Vol. 4 of *Cambridge Studies in Modern Optics,* edited by R. W. Boyd, M. G. Raymer, and L. M. Narducci (Cambridge University Press, Cambridge, England, 1986), p. 240.

[4]W. S. Rabinovich, Ph.D. thesis, Brown University, 1987 (unpublished).

[5]E. H. M. Hogenboom, W. Klishe, C. O. Wiess, and A. Godone, Phys. Rev. Lett. **55**, 2571 (1985).

[6]N. M. Lawandy and D. V. Plant, Opt. Commun. **59**, 55 (1986).

[7]N. M. Lawandy and J. C. Ryan, Opt. Commun. (to be published).

[8]Lloyd W. Hillman, R. W. Boyd, J. Krasinski, and C. R. Stroud, Jr., in *Optical Bistability 2,* edited by K. M. Bowden, H. M. Gibbs, and S. L. McCall (Plenum, New York, 1984), p. 305.

[9]Lloyd W. Hillman, J. Krasinski, R. W. Boyd, and C. R. Stroud, Jr., Phys. Rev. Lett. **52**, 1605 (1984).

[10]Lloyd W. Hillman, J. Krasinski, K. Koch, and C. R. Stroud, Jr., J. Opt. Soc. Am. B **2**, 211 (1985).

[11]C. R. Stroud, Jr., Karl Koch, and Steven Chakmakjian, *Optical Instabilities,* Vol. 4 of *Cambridge Studies in Modern Optics,* edited by R. W. Boyd, M. G. Raymer, and L. M. Narducci (Cambridge University Press, Cambridge, England, 1986), p. 274.

[12]O. Teschke, Andrew Dienes, and John R. Whinnery, IEEE J. Quantum Electron. QE-12, 383 (1976).

[13]F. Y. Wu, R. E. Grove, and S. Ezekiel, Phys. Rev. Lett. **35**, 1426 (1975).

[14]B. R. Mollow, Phys. Rev. **188**, 1969 (1969).

[15]C. R. Stroud, Jr., Phys. Rev. A **3**, 1044 (1972).

[16]B. B. Snavely, in *Dye Lasers,* Vol. 1 of *Topics in Applied Physics,* edited by F. P. Schäfer (Springer-Verlag, New York, 1977), p. 98.

[17]Max Born and Emil Wolf, *Principles of Optics,* 6th ed. (Pergamon, New York, 1980).

[18]W. W. Rigrod, J. Appl. Phys. 36, 2487 (1965).

[19]Lloyd W. Hillman, Jerzy Krasinski, John A. Yeazell, and C. R. Stroud Jr., Appl. Opt. **22**, 3474 (1983).

[20]Karl Koch, Stephen Chakmakjian, Lloyd W. Hillman, and C. R. Stroud, Jr., *Technical Digest of the Annual Meeting of the Optical Society of America, Seattle, 1986* (unpublished), p. 138.

[21]N. M. Lawandy and R. Sohrab Afzal, IEEE J. Quantum Electron. QE-22, 2251 (1986).

[22]S. Schrotter and D. Kuhlke, Opt. Quantum Electron. **13**, 256 (1985).

[23]I. A. Kotomtseva, N. A. Loiko, and A. M. Samson, J. Opt. Soc. Am. B **2**, 232 (1985).

[24]P. A. Khandokhin and Ya. I. Khanin, J. Opt. Soc. Am. B **2**, 226 (1985).

[25]C. L. Tang, H. Statz, and G. deMars, Appl. Phys. Lett. **2**, 222 (1963).

[26]H. Kogelnik and C. V. Shank, J. Appl. Phys. **43**, 2327 (1972).
[27]S. R. Chinn, IEEE J. Quantum Electron. QE-9, 578 (1983).
[28]William Streifer, Robert D. Burnham, and Donald R. Scifres, IEEE J. Quantum Electron. QE-11, 158 (1975).
[29]W. S. Rabinovich and N. M. Lawandy, IEEE J. Quantum Electron. QE-23, 234 (1987).
[30]Murray Sargent III, William H. Swantner, and John D. Thomas, IEEE J. Quantum Electron. QE-16, 465 (1980).

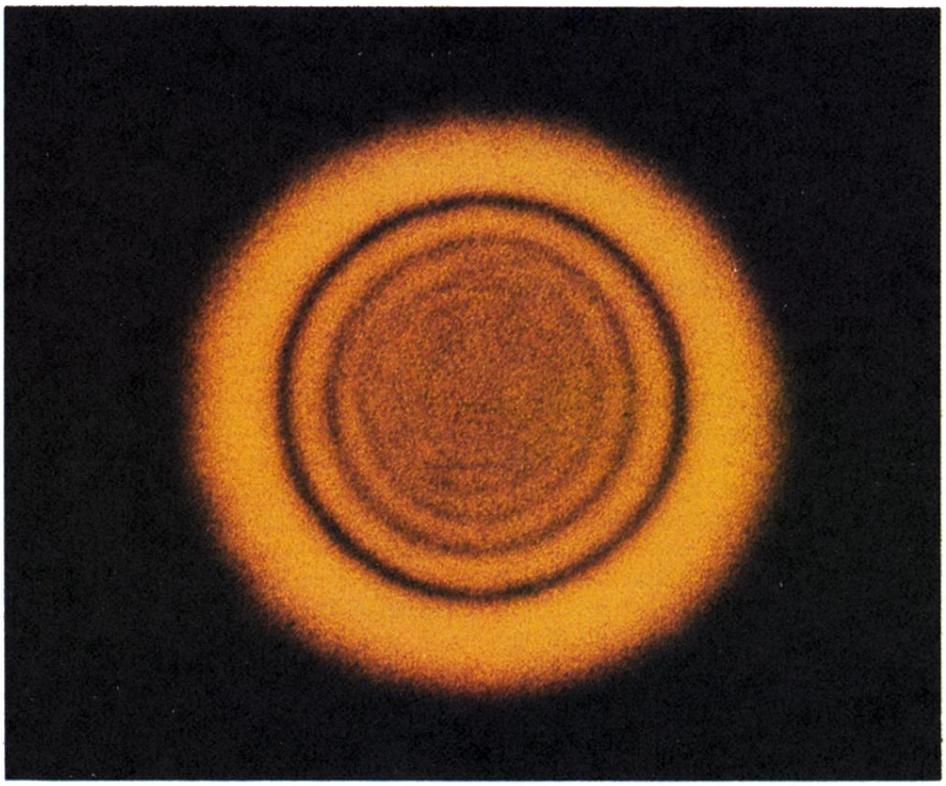

FIG. 6. Newton's rings formed by the thermal lensing effect when the laser was in its lowest-order transverse mode and operating bidirectionally with an 80-Å splitting.